ARTICLE
Journal of Cellular Biochemistry 116:2744–2754 (2015)

Journal of Cellular Biochemistry

Effects of Novel ncRNA Molecules, p15-piRNAs, on the Methylation of DNA and Histone H3 of the CDKN2B Promoter Region in U937 Cells

Dansen Wu,[1,2] Haiying Fu,[1] Huarong Zhou,[1] Junnan Su,[1] Feng Zhang,[1] and Jianzhen Shen[1]*

[1]*Department of Hematology, Union Hospital of Fujian Medical University, Fujian Institute of Hematology, Fuzhou, Fujian 35001, China*

[2]*Medical Intensive Care Unit, Fujian Provincial Hospital, Fuzhou, Fujian 35001, China*

ABSTRACT

Non-coding RNAs (ncRNAs) play key roles in epigenetic events. However, the exact mechanism of ncRNA guidance, particularly piwi-interacting RNAs (piRNAs), for the targeting of epigenetic regulatory factors to specific gene regions is unclear. Although piRNA function was first established in germ-line cells, piRNA may be crucial in cancer cells. This study investigated the potential roles of *CDKN2B*-related piRNA in leukemia cells to provide a potential tumorigenesis model of leukemia. *CDKN2B*-related piRNAs, hsa_piR_014637 and hsa_piR_011186 were transduced into the leukemia cell line U937 to study the effect of these two piRNAs on cell-cycle progression, apoptosis, heterochromatin formation, CDKN2B methylation and expression. Our results show that over-expressing hsa_piR_011186 promoted cell-cycle progression and decreased apoptosis. We also observed inhibition of *CDKN2B* gene expression. These effects were likely mediated by novel piRC (piRNA complex) of *CDKN2B*-related piRNA that associate with DNMT1, Suv39H1 and/or EZH2 proteins to modulate the methylation of DNA and histone H3 in the promoter region of the *CDKN2B* gene. The novel piRC complex facilitated epigenetic modifications on the promoter of cell-cycle regulating genes, providing an expanded view of the role of piRNA in the progression of leukemia cells. J. Cell. Biochem. 116: 2744–2754, 2015.

KEY WORDS: ACUTE LEUKEMIA; EPIGENETICS; piRNA COMPLEX (piRC); NON-CODING RNA; CDKN2B GENE; DNA METHYLATION; HISTONE MODIFICATION

Epigenetics is the study of inheritable modifications of gene expression and regulation without changes to the original DNA sequence. These modifications include DNA methylation, histone modification, genomic imprinting, and small molecule RNA-related gene silencing.

Piwi-interacting RNAs (piRNAs) are non-coding RNAs (ncRNAs) [Aravin et al., 2006] endogenously expressed in mammalian testes. They belong to a distinct class of small ncRNAs and form piRNA-induced silencing complex (piRISC) in the germ cells of many species. Under physiological conditions, piRNA and the Piwi family of proteins interact to form piRNA complexes (piRCs) [Girard et al., 2006; Grivna et al., 2006; Lau et al., 2006] to maintain the integrity of the genome by silencing transposable elements [Siomi et al., 2011]. piRNAs mediate the methylation of transposon DNA in mice [Shirayama et al., 2012; Leslie, 2013] and is the specific determinant of DNA methylation in germ cells [Bourc'his and Bestor, 2004; Chen et al., 2012].

Argonaute proteins are divided into the Ago subfamily and the Piwi subfamily. They are found in multiple species and are known to play essential roles in the production and targeting of ncRNAs [Wei

Conflict of interest: None.

Grant sponsor: Fujian Medical University; Grant number: 09-ZD021; Grant sponsor: National Natural Science Foundation of China; Grant number: 81370629 and 81300428; Grant sponsor: Natural Science Foundation of Fujian Province; Grant number: 2011J01179; Grant sponsor: Fujian Provincial Health Bureau Youth Research Projects; Grant number: 2010-1-12; Grant sponsor: National Clinical Key Specialty Construction Project.

*Correspondence to: Dr Jian-Zhen Shen, Fujian Institute of Hematology, Union Hospital, Fujian Medical University, Fuzhou, Fujian 350001, P.R. China.
E-mail: jianzhenshen@yeah.net

Manuscript Received: 26 October 2014; Manuscript Accepted: 14 April 2015

Accepted manuscript online in Wiley Online Library (wileyonlinelibrary.com): 23 July 2015

DOI 10.1002/jcb.25199 • © 2015 Wiley Periodicals, Inc.

et al., 2013]. For example, human AGO2 protein is the core element of the RISC and engages in targeted mRNA cleavage, translation inhibition and chromatin modification. In fission yeast in which the AGO and Dicer genes have been knocked-down, it was determined that the transcriptional-silencing of repeating sequences in the centromere was through the methylation of histone H3 at lysine 9 by Swi6, thus regulating gene expression at the transcript level [Lippman and Martienssen, 2004]. Similar to fission yeast, AGO proteins in human cells are also crucial for the RNA interference-mediated heterochromatinization and subsequent transcriptional silencing [Morris, 2008]. In *Drosophila*, AGO3, a member of the Piwi subfamily, participates in the generation of piRNAs and mediate silencing of gene expression through heterochromatin formation [Zaratiegui and Martienssen, 2012].

Although piRNAs have been previously suggested to be germline-specific, recent studies have shown that they also play crucial roles in nongonadal cells [Ishizu et al., 2012]. It was presumed that piRNA pathways evolved specifically in germ cells to defend against the invasion of external genetic elements and to maintain cellular genetic integrity and stability. Recent studies have shown that piRNAs may play a role in cancer biogenesis [Cheng et al., 2011]. Hiwi, one of the four PIWI proteins found in humans, associates with piRNAs. Through an epigenetic process, they might contribute to the stem cell-like epigenetic state of cancer progression. Although aberrant expression of piRNA has been detected in tumor tissues including cervical, gastric, colonic, mammary and lung cancers [Cheng et al., 2011; Lu et al., 2011; Cheng et al., 2012; Siddiqi and Matushansky, 2012], its expression level in leukemia cell has not been studied.

Acute leukemia (AL) is a group of heterogeneous clonal disease induced by mutations in hematopoietic stem cells and/or hematopoietic progenitor cells, resulting in hematopoietic malignancy. While the exact mechanism remains unknown, a correlation exists between abnormal epigenetic modifications on certain chromosomes and the onset of leukemia progression [Foltankova et al., 2012]. The expression of CDK inhibitor is down-regulated in human sarcomas as a result of Hiwi-mediated DNA methylation [Siddiqi et al., 2012]. In some cases of leukemia, such as chronic myeloid leukemia, multiple myeloma, and lymphoma, the promoter region of the INK4 (inhibitors of cyclin-dependent kinase 4) family member *CDKN2B* gene is hyper-methylated, suggesting that hyper-methylation of *CDKN2B* plays a crucial role in the genesis and progression of certain hematopoietic malignancies [Takeuchi et al., 1995; Kusy et al., 2004; Papageorgiou et al., 2007; Bies et al., 2010]. Not surprisingly, *CDKN2B* encoded protein P15INK4B is involved in regulating cell growth and inhibiting cell cycle progression.

The Piwi proteins of piRC mediate the covalent modification of euchromatic histone, which results in the heterochromatinization of telomere-associated sequence on the right arm of chromosome 3 (3R-TAS) and activates the piRNA transcription in the site [Yin and Lin, 2007]. The "Piwi-piRNA guidance hypothesis" was formulated to describe the epigenetic functions of piRNA, suggesting that Piwi-piRNA complex function to recognize specific target sequence and recruite epigenetic effectors, such as heterochromatin protein 1a (HP1a) to those targets [Brower-Toland et al., 2007; Yin and Lin, 2007; Halic and Moazed, 2009; Ashe et al., 2012; Le Thomas et al., 2013]. The sequence complementarity between the piRNA and the target sequence is an important determinant of the regulatory mechanism [Ender and Meister, 2010].

In this study, we aimed to investigate how piRNA regulate the expression of p15, a CDK inhibitor (CDKI), through epigenetic modification in U937 leukemia cells. Two *CDKN2B* gene-related piRNAs, piR_014637 and piR_011186, located within the 6411 nucleotide CDKN2B gene, are endogenously expressed in U937 cells. Using a lentiviral vector expression system, these piRNAs were overexpressed, to enable identification of binding proteins with epigenetic modification activity. Our novel findings suggest a piRC-mediated inhibition of p15 CDKI as a potential mechanism of tumorigenesis in hematopoietic cells.

MATERIALS AND METHODS

CELL CULTURE

Acute myeloid leukemia cell line U937 (CRL-1593.2™; ATCC, Manassas, VA) was obtained from the Fujian Institute of Hematology. Cells were grown in 7–10 mL of RPMI-1640 (Gibco, Carlsbad, CA) supplemented with 10% fetal calf serum (Sijiqing, Zhejiang, China) at 37°C in a humidified incubator containing 5% CO_2. Cells in logarithmic growth phase were subjected to further study.

IDENTIFICATION AND ANALYSIS OF piRNA COMPLEX MEMBERS

Universal Magnetic Co-IP kit (Active Motif, Carlsbad, CA) was applied to identify members of the piRNA complex in U937 cells. Five target protein detection groups (Enhancer of Zeste homolog2 (EZH2), suppressor of variegation 3–9 homolog 1(Suv39H1), DNA methyl transferase 1 (DNMT1), DNA methyltransferase 3a (DNMT3a), and DNA methyltransferase 3b (DNMT3b)) and nuclear extract group were set in each Co-IP operation. Cells (5×10^6) in logarithmic growth phase were taken for nuclear extract preparation in each group. Nuclear extract (400–500 μg) and 5 μg monoclonal antibody to each protein group member (Active Motif) were combined in a final volume of 500 μL with complete Co-IP/Wash Buffer in a pre-chilled 1.5 mL microcentrifuge tube and incubated for 4 h at 4°C on a three-dimensional orbital shaker (Kylin-Bell Lab Instruments, Haimen, China). Twenty-five microliters of Protein G magnetic beads were added to each tube and incubated for 1 h at 4°C on a rotator. Afterwards, tubes were placed on magnetic stand to pellet beads on the side of the tube. The supernatant was carefully removed from each tube and discarded, then 500 μL Complete Co-IP/Wash Buffer was added to resuspend the pellet completely by pipetting up and down several times. Finally, piRC member AGO3 protein in the six aforementioned samples and a blank control were analyzed by Western blotting with RIPAb+™ Ago3 monoclonal antibody (♯03–250; Millipore, Billerica, MA) as primary antibody and horseradish peroxidase-labeled goat anti-mouse IgG antibody (Golden Bridge, Peking, China) as secondary antibody.

CELL TRANSDUCTION

The nucleotide sequences of hsa_piR_014637(Minus:UGGUCUC-GAACUCCUGACCUCAGGUGAUCU) and hsa_piR_011186 (Plus:

UGCCUGUAAUCCCAGCACUUUGGGAGGCC) (retrieved from the piRNA database; http://pirnabank.ibab.ac.in/) were sub-cloned into the lentiviral GV209 vector, and the respective expression plasmids LV-hsa_piR_014637 and LV-hsa_piR_011186 were constructed for the overexpression of piRNAs (cat. ♯ GMUL30566 and GMUL30569; Genechem, Shanghai, China). The virus titers were 1.5×109 and 1.2×109 transducing units/mL, respectively. U937 cells in logarithmic growth phase were divided in GV209 vector transduction group, LV-hsa_piR_014637 and LV-hsa_piR_011186 transduction groups. Each transduction group containing $2–4 \times 105$ cells was incubated at 37°C in a humidified incubator containing 5% CO2. The next day, poly-L-lysine was added to a final concentration of 6 μg/mL to each group and $4–6 \times 106$ viral units were added after 30 min. The transduction efficiency was determined 48 h later.

ANALYSIS OF piRNA EXPRESSION LEVELS

According to the piRNA sequences related to the *CDKN2B* gene, hsa_piR_014637 and hsa_piR_011186, specific primers and PCR Fluorescence Quantitative Detection Kit for reverse transcription were purchased (ABI, San Francisco, California). Transduced cells were incubated for 48 h, and cells in logarithmic growth stage were collected. Total cell number was approximatedly 2×10^6. RNA was purified using TRIzol and the purified total RNA was subjected to reverse transcription reaction using TaqMan® MicroRNA Reverse Transcription Kit (ABI). An ABI7500 Real-Time RCR module, TaqMan® Universal PCR Master Mix II ($2\times$) with UNG kit and TaqMan® Small RNA Assay ($20\times$) were employed for real-time quantitative polymerase chain reaction (qPCR) analysis of RNA reverse transcription products, with U1 snRNA as internal control. The total reaction volume was 20 μL, including 10 μL Master Mix, 1.33 μL cDNA, 1.0 μL Small RNA Assay and 7.67 μL RNAse-free H_2O. The reaction condition were 50°C, 2 min for 1 cycle (1st stage), 95°C, 10 min for 1 cycle (2nd stage) followed by 40 cycles of 95°C for 15 sec and 60°C for 60 sec (3rd stage). Every reaction mixture was run in triplicate. ΔCt value comparison was used to evaulate the expression levels of hsa_piR_011186 and hsa_piR_014637 molecules. The algorithm was: ΔCt = Ct value (piRNA)-Ct value (U1 snRNA), ΔΔCt = ΔCt (transduction group)-ΔCt (control group), relative quantification (RQ) of transduction group $= 2^{-\Delta\Delta Ct}$ and the RQ of control group set to 1.

RNA IMMUNOPRECIPITATION (RIP)-qLPCR ANALYSIS

Transduced cells were incubated for 48 h and cells in logarithmic growth phase were collected (approximately 1.0×10^7 cells). Magna RIP™ RNA-Binding Protein Immunoprecipitation Kit (Millipore) and RIPAb + ™ Ago3 monoclonal antibody (♯03–250; Millipore) were utilized to analyze cellular RIP-qPCR products. Each transduction group was performed in triplicate. Based on the designed primers for reverse transcription and real-time PCR kit instructions, a TaqMan® MicroRNA Reverse Transcription Kit (ABI) was used for RNA reverse-transcription reactions. ABI7500 Real-Time RCR module, TaqMan® Universal PCR Master Mix II ($2\times$) with UNG kit and TaqMan® Small RNA Assay ($20\times$) were employed for real-time qPCR analysis of piRNA reverse transcription products, with U1 snRNA as internal control. The total reaction volume was 20 μL, including 10 μL Master Mix, 1.33 μL cDNA, 1.0 μL Small RNA Assay and 7.67 μL RNAse-free H_2O. The reaction conditions were 50°C, 2 min for 1 cycle (1st stage), 95°C, 10 min for 1 cycle (2nd stage) followed by 40 cycles of 95°C, 15 sec, and 60°C, 60 sec (3rd stage). Every reaction mixture was performed in triplicate. Values for analysis were represented by the percent of input and fold-change. The standardized RNA amounts were calculated as $\Delta Ct_{\text{normalized ChIP}} = Ct_{ChIP}\text{-}[Ct_{Input}\text{-}Log2^{(\text{Input Dilution Factor})}]$, Input Dilution Factor $=$ (fraction of the input chromatin) $^{-1} = (1\%)^{-1} = 100$; $\%\text{Input} = 2^{-\Delta Ct_{\text{normalized ChIP}}} \times 100\%$; Fold Change $= 2^{-\Delta\Delta Ct}$. $\Delta\Delta Ct = \Delta Ct_{\text{normalized ChIP transcription group}} - \Delta Ct_{\text{normalized ChIP control group}}$.

CELL CYCLE AND APOPTOSIS ANALYSIS

The proliferation rates of the three transduced groups were inspected using CCK-8 solution (Dojindo). 2,500 cells were seeded on 96-well plates. After treatment for 48 h, 10 μL CCK-8 solution was added to each well and cells were incubated for 2 h at 37°C, then the absorption values at 450 nm were measured. Cell proliferation and apoptosis were evulated by double staining with fluorescein isothiocyanate (FITC) and propidium iodide (PI). Each experiment was done in triplicate.

ANALYSIS OF CDKN2B GENE EXPRESSION LEVEL

Transduced cells were incubated for 48 h, and cells in logarithmic growth stage were collected (approximately 2×10^6 cells). RNA was purified using TRIzol and purified total RNA was used to synthesize the 1st strand of CDKN2B cDNA using a Reverse Transcription Kit (Fermentas, Waltham, Massachusetts). An ABI7500 Real-Time RCR module and FastStart Universal SYBR Green Master (ROX) kit were employed to investigate reverse-transcription products using glyceraldehyde-3-phosphate dehydrogenase (GADPH) as the internal control. The total reaction volumn was 20 μL, including 10 μL of SYBR®-Green Master, 1 μL cDNA, 0.3 μL of forward and reverse primers each (20 μM), 0.8 μL of UNG (1U/μL) and 7.6 μL RNAse-free H_2O. The reaction conditions were 50°C, 2 min for 1 cycle (1st stage), 95°C, 2 min for 1 cycle (2nd stage) followed by 95°C, 15 sec then 60°C, 60 sec for 40 cycles (3rd stage). Melting curve analysis involved one cycle each of 95°C, 15 sec; 60°C, 60 sec; 95°C, 15 sec then 60°C, 15 sec. Every reaction mixture was run in triplicate and qPCR was also applied in triplicate for all cell groups. Ct values indicate the expression levels of CDKN2B mRNA, and ΔCt = Ct (CDKN2B)-Ct(GAPDH), ΔΔCt = ΔCt(transduction group)-ΔCt(control group); the RQ of transduction group $= 2^{-\Delta\Delta Ct}$ and the RQ of control group was set to 1. p15 polyclonal antibody and GAPDH monoclonal antibody were utilized to show the $p15^{INK4b}$ protein expression in U937 cells by Western Blot.

ANALYSIS OF CpG ISLAND METHYLATION IN THE PROMOTER REGION

The sequence data of CDKN2B gene promoter region (Accession Number 42920) was retrieved from Transcriptional Regulatory Element Database (http://rμLai.cshl.edu/cgi-bin/TRED/tred.cgi?process=home). BSP primers were designed (Table I) by Methyl Primer Express v1.0 software (ABI). The synthesis and purification were performed by Invitrogen Cnservice (Shanghai, China). Transduced cells were incubated for 48 h, and cells in logarithmic growth stage were collected (approximately 2.0×10^6 cells).

TABLE I. Primer Sequences

Primers	Sequence (5′→3′)	Tm value (°C)	Product length (bp)
BSP			
Forward	TTTATTGGGGATTAGGAGTTGA	60.87	
Reverse	CTCCTTCCTAAAAAACCTAAACTCA	61.15	543
ChIP-qPCR			
Forward	CCTGGATTGCTTCTGGGAAAAAG	60.06	
Reverse	AGCTGAAAACGGAATTCTTTGCC	60.55	154
ChIP-qPCR control			
Forward	AAGATTCTAGGACTCAACTCATT	60.9	
Reverse	GGATTACAGACATAAGCCACT	61.4	170

Genomic DNA was extracted by conventional chloroform method, followed by bisulfite conversion and purification with Epitech Bisulfite Kit (Qiagen, Hilden, Germany). Converted DNA was analyzed by BSP. The PCR reaction mix contained 25 μL of 2 × GoldStar Best Master Mix, 5 μL of bisulfite-converted DNA, 1 μL for both forward and reverse primers (20 μM) and RNAse-free H_2O to a total volume of 50 μL. Reaction conditions were pre-denaturation at 95°C, 10 min, denaturation at 95°C, 40 sec, cool-down to 50°C for 50 sec andextension at 72°C for 60 sec. After a total of 40 cycles, the reaction was stopped after additional extension at 72°C for 10 min. The PCR products were cloned and sequenced by Invitrogen (Shanghai, China). Each cell group and control products were cloned and sequenced 10 times. EpiTect Control DNA and Control DNA Set (Qiagen) served as positive and negative controls for the specificity of methylation, respectively. Once the cloned sequences were obtained, BiQ Analyzer 2.0 DNA methylation analysis software was employed to investigate the CpG island methylation, the methylation percentage in each locus, and sequence comparison and point charts were drawn.

CHROMATIN IMMUNOPRECIPITATION (ChIP)-qPCR ANALYSIS

The aforementioned CDKN2B promoter sequence (Accession Number 42920) was used to design qPCR primers using Beacon Designer 7 software (PREMIER Biosoft, Palo Alto, California), which were synthesized and purified by Invitrogen Cnservice. Transduced cells were incubated for 48 h and cells in logarithmic growth stage were collected (approximately 1.0×10^7 cells). EZ-Magna ChIP™ A/G One-Day Chromatin Immunoprecipitation Kits (catalog♯ 17–10086; Millipore) were used for ChIP-qPCR analysis. Cell harvesting, sonication, chromosome immunoprecipitation, washing of the precipitated complex and de-crosslinking procedures were performed strictly following the provided protocol. De-crosslinked products (DNA segments) were purified by chloroform/glycogen method (Thermo Scientific, Pittsburgh, PA). The qPCR reaction mix for DNA segments contained 10 μL SYBR®-Green Master, 2 μL DNA solution, 0.3 μL forward and reverse primers each (20 μM), 0.8 μL UNG (1 U/μL) and 6.6 μL RNAse-free H_2O. Reaction conditions were 50°C, 2 min, 1 cycle (1st stage); 95°C, 2 min, 1 cycle (2nd stage); 40 cycles of 95°C, 15 sec and 60°C, 60Nsec (3rd stage); for melting curve analysis, 95°C, 15 sec, 60°C, 1 min, 95°C, 15 sec, 60°C, 15 sec for 1 cycle. Every reaction mixture was performed in triplicate, as was ChIP-qPCR for all cell groups. The analysis of qPCR results and the standardization of DNA amounts were represented as "% input" and "fold change": $\Delta Ct_{\text{normalized ChIP}} = Ct_{ChIP}\text{-}[Ct_{Input}\text{-}Log_2{}^{(\text{Input Dilution Factor})}]$, Input Dilution Factor = (fraction of the input chromatin)$^{-1}$ = (1%)$^{-1}$ = 100; %Input = $2^{-\Delta Ct\ \text{normalized ChIP}} \times 100\%$; Fold Change = $2^{-\Delta\Delta Ct}$. $\Delta\Delta Ct = \Delta Ct_{\text{normalized ChIP transduction group}} - \Delta Ct_{\text{normalized ChIP control group}}$.

STATISTICAL ANALYSIS

Continuous data were expressed as mean ± standard deviation (SD). Due to small sample size (n = 3) and the lack of normal hypothesis, all paired comparisons were perfomed with Mann–Whitney U test. A *P*-value under 0.05 would be recognized as reaching significance of each test. All analyses were performed using IBM SPSS Version 19 (SPSS Statistics V19, IBM Corporation, Somers, New York).

RESULTS

ENDOGENOUS AND OVER-EXPRESSION OF piRNAs IN U937 LEUKEMIA CELLS

This study investigated piRNA regulated expression of p15, a CDK inhibitor, in U937 leukemia cells. To detect *CDKN2B* (which encodes the p15 protein) gene-related piRNAs, we used piRNABANK (http://pirnabank.ibab.ac.in/) to search for piRNAs in the vincinity of the *CDKN2B* gene. The gene is located on chromosome 9, at position 21992901 to 21999311. The piRNABANK search revealed four candidate results including two potential piRNAs: a 30-nucleotide, minus strand piR_014637, and a 29-nucleotide, plus strand piR_011186. Both piRNAs are located within the 6411 nucleotide *CDKN2B* gene. Both piRNAs are endogenous in U937 cells. Secondary structure prediction tool in the piRNA DATABASE showed that both piRNAs exhibit typical piRNA features (Fig. 1a). To assess the expression levels of hsa_piR_011186 and hsa_piR_014637 in U937 and transduced cells, qPCR was performed. In U937 cells, levels of hsa_piR_011186 were higher than hsa_piR_014637 ($P = 0.050$) (Fig. 1b). After transduction of hsa_piR_011186 and LV-hsa_piR_014637, both piRNA levels increased (Fig. 1c), and no significant difference was detected in the expression level of the two piRNAs ($P = 0.38$). Using the lentiviral vector expression system, these piRNAs were overexpressed in U937 cells in subsequent studies.

CELL PROLIFERATION AND APOPTOSIS PROFILES OF TRANSDUCED CELLS

By overexpressing hsa_piR_011186 and hsa_piR_014637 in U937 cells, we were able to observe an amplification of the biological

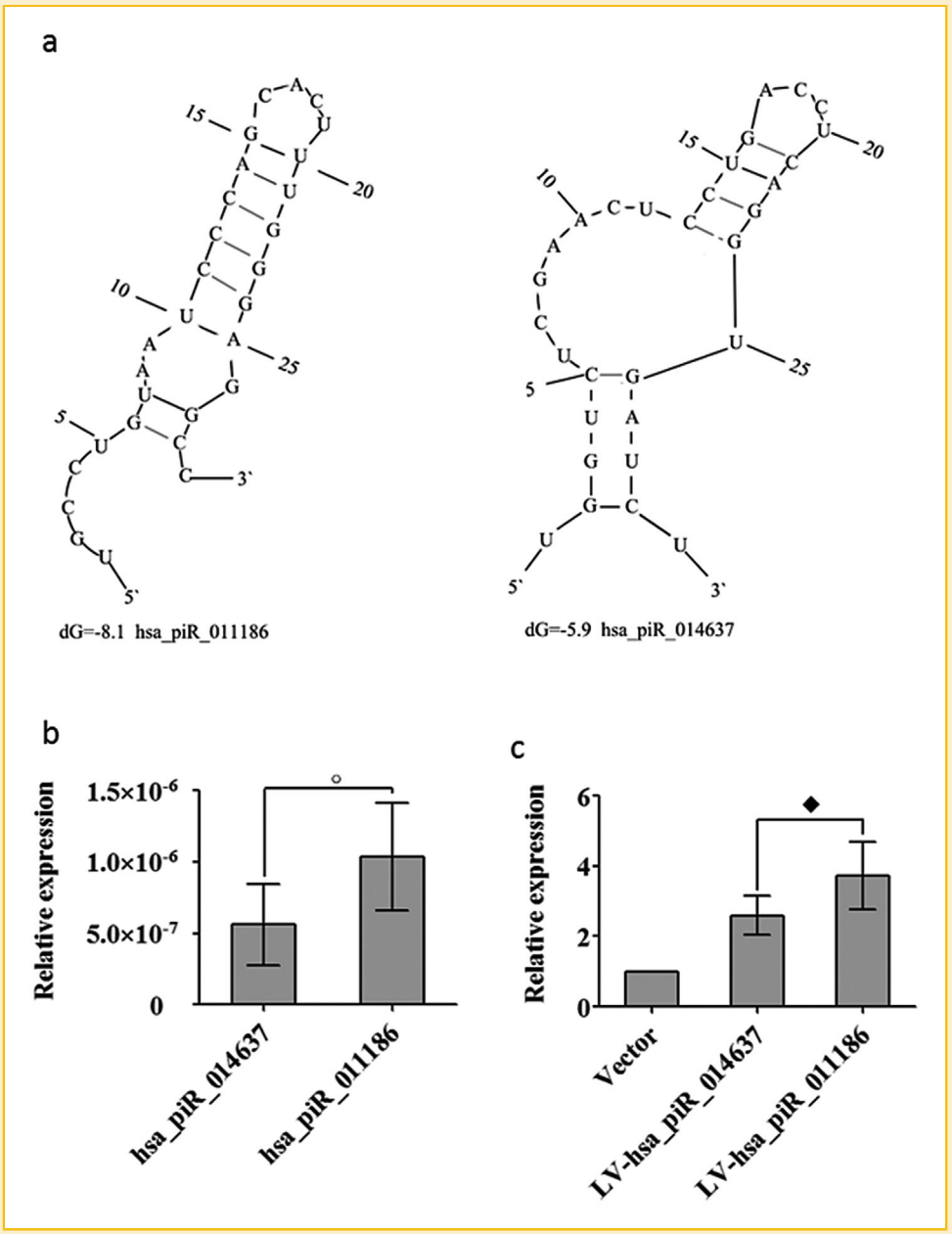

Fig. 1. piR_011186 and piR_014637 secondary structure and expression in U937 human leukemia cells. (a) By the on-line piRNA structure prediction tool (http://pirnabank.ibab.ac.in/UNAFold/unahome.cgi), the predicted structures of both piRNAs showed typical features of piRNAs. (b) RNA was prepared and assayed for hsa_piR_014637 and hsa_piR_011186 expression in U937 human leukemia cells. Relative expression of individual piRNA was normalized by U1 snRNA. The results represent mean ± standard deviation of three independent experiments performed in triplicate. (c) U937 cells were infected with vector, LV-hsa_piR_014637 or LV-hsa_piR_011186 for 48 h. RNA was assayed for hsa_piR_014637 and hsa_piR_011186 expression. The results represent mean ± standard deviation of three independent experiments performed in triplicate. Mann–Whitney U test, ○ represents $P \leq 0.05$, hsa_piR_014637 vs hsa_piR_011186 in U937 cells. ◆ represents $P > 0.05$ LV-hsa_piR_011186 group vs hsa_piR_014637.

functions of these piRNAs. Here, we assayed cell proliferation and apoptosis using cck-8 cell proliferation testing and Annexin V-FITC/PI double staining, respectively. Both piRNAs enhanceed cell proliferation (Fig. 2a), while only piR_011186 significant facilitated the entry into the S-phase of the cell cycle (2b). In hsa_piR_011186 tranduced cells, we observed inhibition of apoptosis, suggestive of a role of hsa_piR_011186 in tumor biogenesis (Fig. 2c).

CDKN2B GENE EXPRESSION IN TRANSDUCED CELLS

To delineate whether piRNA down-regulated CDKN2B expression, we used qPCR and Western blot to scrutinize the gene expression level in transduced cells. After transduction with lentiviral plasmid, the CDKN2B mRNA level and p15 protein level in U937 cells were significantly down-regulated in the LV-hsa_piR_011186-transduced group ($P = 0.05$), but not in the LV-hsa_piR_014637-transduced group (Fig. 3).

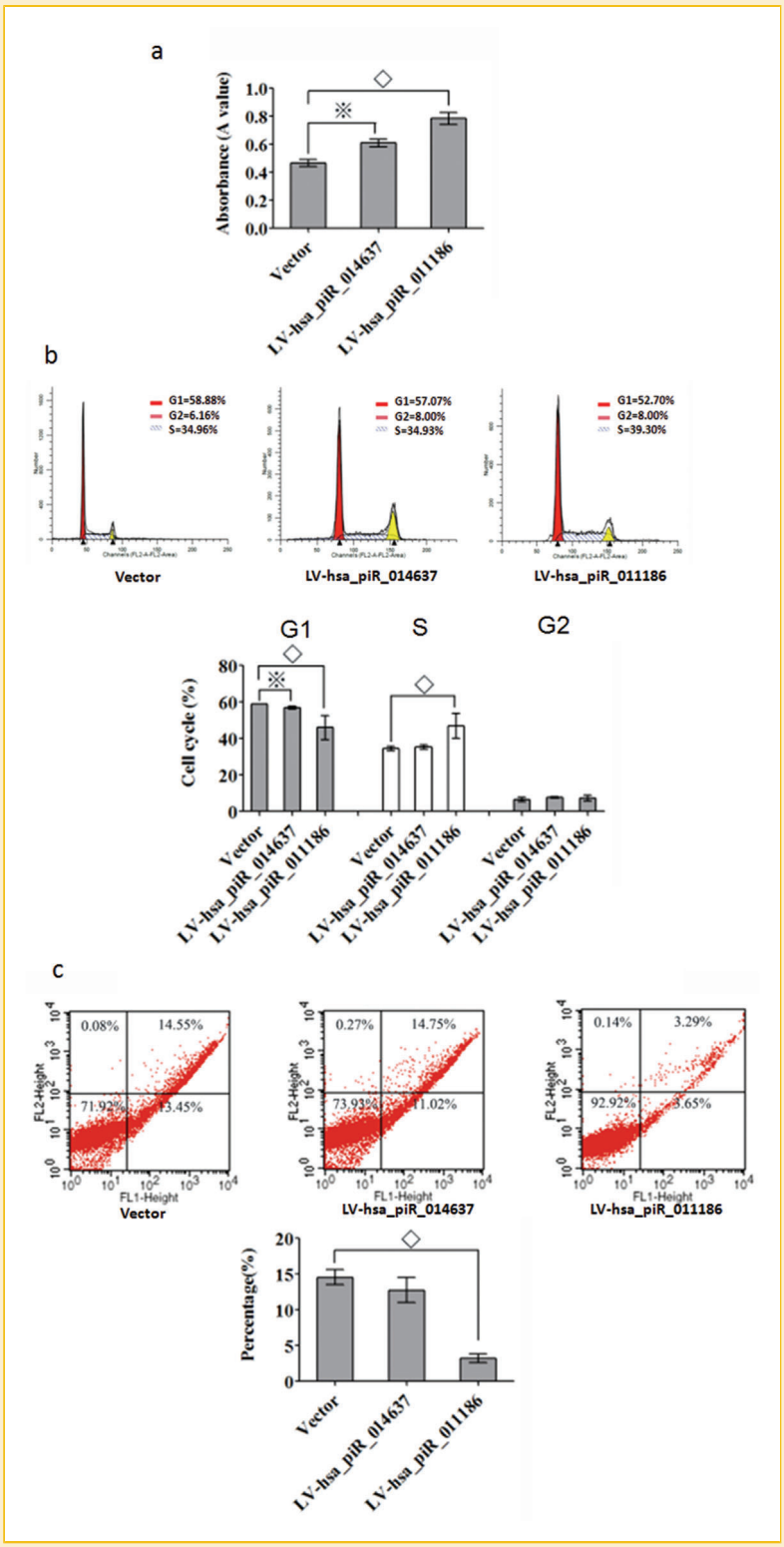

Fig. 2. Evaluation of the viability and apoptotic events in U937 human leukemia cells infected with vector, LV-hsa_piR_014637 or LV-hsa_piR_011186. U937 cells were infected with vector, LV-hsa_piR_014637 or LV-hsa_piR_011186 for 48 h. (a) For cell viability assay, CCK8 was added and 2 h later, viability was assessed by spectrophotometry at 450 nm. The results represent mean ± standard deviation of three independent experiments performed in triplicate. Mann–Whitney U test, ※ represents $P \leq 0.05$, LV-hsa_piR_014637 group vs vector control group. ◇ represents $p \leq 0.05$, LV-hsa_piR_011186 groupvs vector control group. (b) Cell cycle was analyzed by flow cytometry. The results represent mean ± standard deviation of three independent experiments. Mann–Whitney U test, ※ represents $P \leq 0.05$, LV-hsa_piR_014637 group vs Vector control group. ◇ represents $P \leq 0.05$, LV-hsa_piR_011186 group vs Vector control group. (c) Cell apoptosis was assessed using Annexin V-FITC/PI. The results represent mean ± standard deviation of three independent experiments. Mann-Whitney U test, ◇ represents $P \leq 0.05$, LV-hsa_piR_011186 groupvs vector control group.

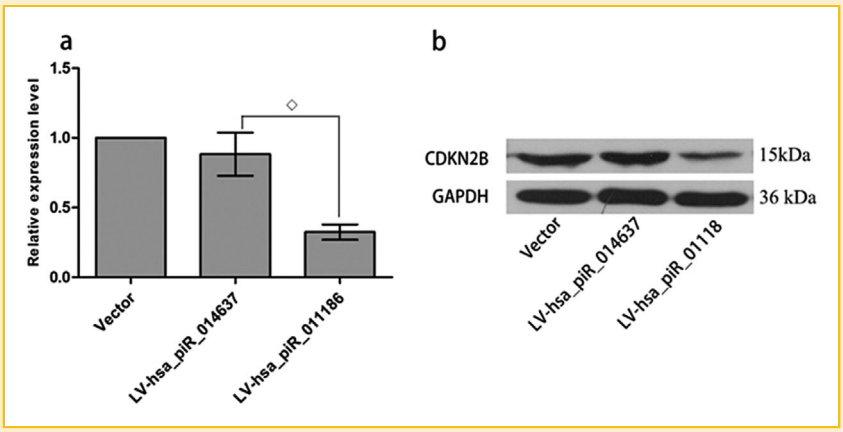

Fig. 3. Expression levels of the CDKN2B gene in U937 human leukemia cells after infection. (a) U937 cells were infected with Vector, LV-hsa_piR_014637 or LV-hsa_piR_011186 for 48 h. After transfecttion, RNA was prepared and assayed for CDKN2B mRNA expression in U937 cells. Relative expression of individual CDKN2B mRNA was normalized by GAPDH mRNA. The results represent mean ± standard deviation of three independent experiments. Infected groups RQ = $2^{-\Delta\Delta Ct}$, vector control group RQ = 1. Mann-Whitney U test, ◇ represents $P \leq 0.05$, LV-hsa_piR_011186 group vs LV-hsa_piR_014637 group. (b) Total cell lysates were collected after infection of U937 cells with vector, LV-hsa_piR_014637 or LV-hsa_piR_011186 for 48 h and subjected to Western blotting. The membranes were probed with anti-CDKN2B Ab (top panel), or anti-GAPDH Ab (lower panel). Representative data for three separate experiments are shown.

DNA METHYLATION PROFILE WITHIN THE PROMOTER REGION OF CDKN2B IN TRANSDUCED CELLS

Over-expression of LV-hsa_piR_011186 piRNAs correlated with the down-regulation of CDKN2B mRNA and p15 protein expression. Since the methylation of a gene's promoter region could lead to gene down-regulation, it was necessary to examine the methylation level in the promoter region of CDKN2B in transduced U937 cells. The BSP assay was used to investigate the methylation profile for 45 sites in

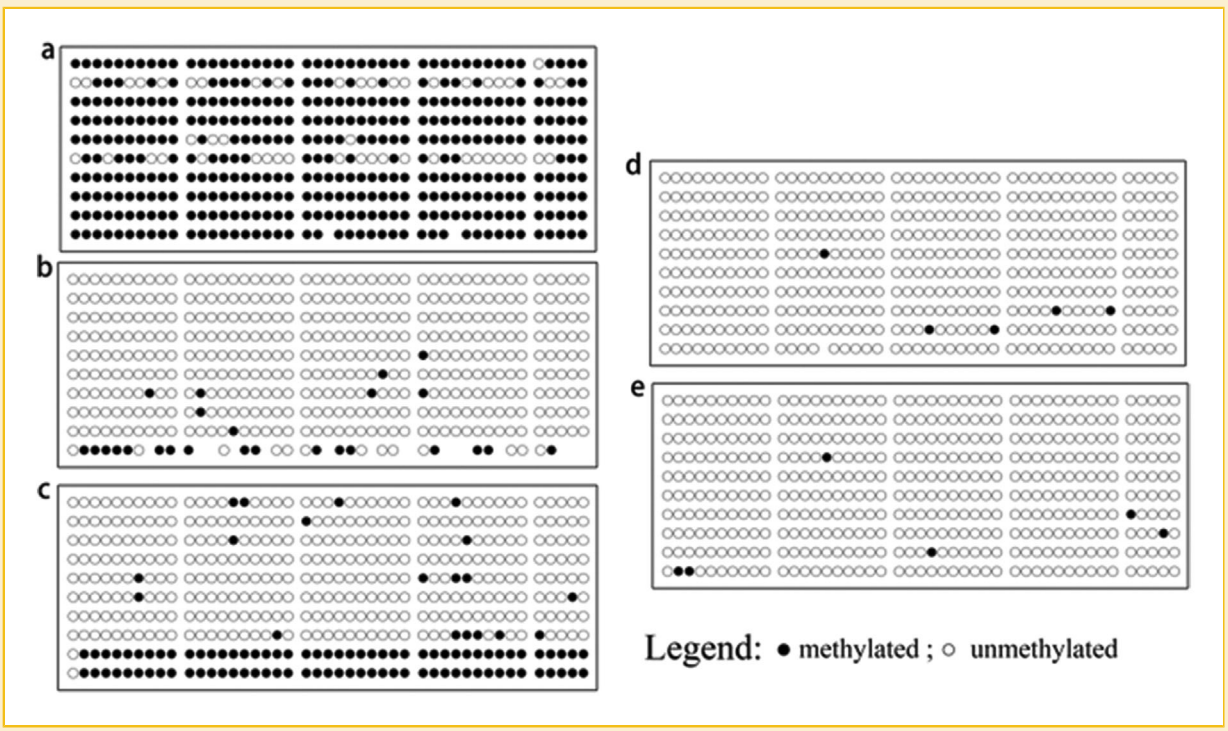

Fig. 4. Point charts of DNA methylation of CDKN2Bgene promoter in U937 human leukemia cells after infection. (a) Human bisulfite converted methylated control DNA. (b) Human bisulfite converted unmethylated control DNA. (c) In the LV-hsa_piR_011186 infection group there were abnormal methylations in CG sites of CDKN2Bgene promoter in U937 cells. Methylation rates among 2 to 44CG sites were different. (d)In LV-hsa_piR_014637 infection group there were no methylations in CG sites of CDKN2B gene promoter in U937 cells. (e) In vector control infection group there were no methylations in CG sites of CDKN2B gene promoter in U937 cells as well.

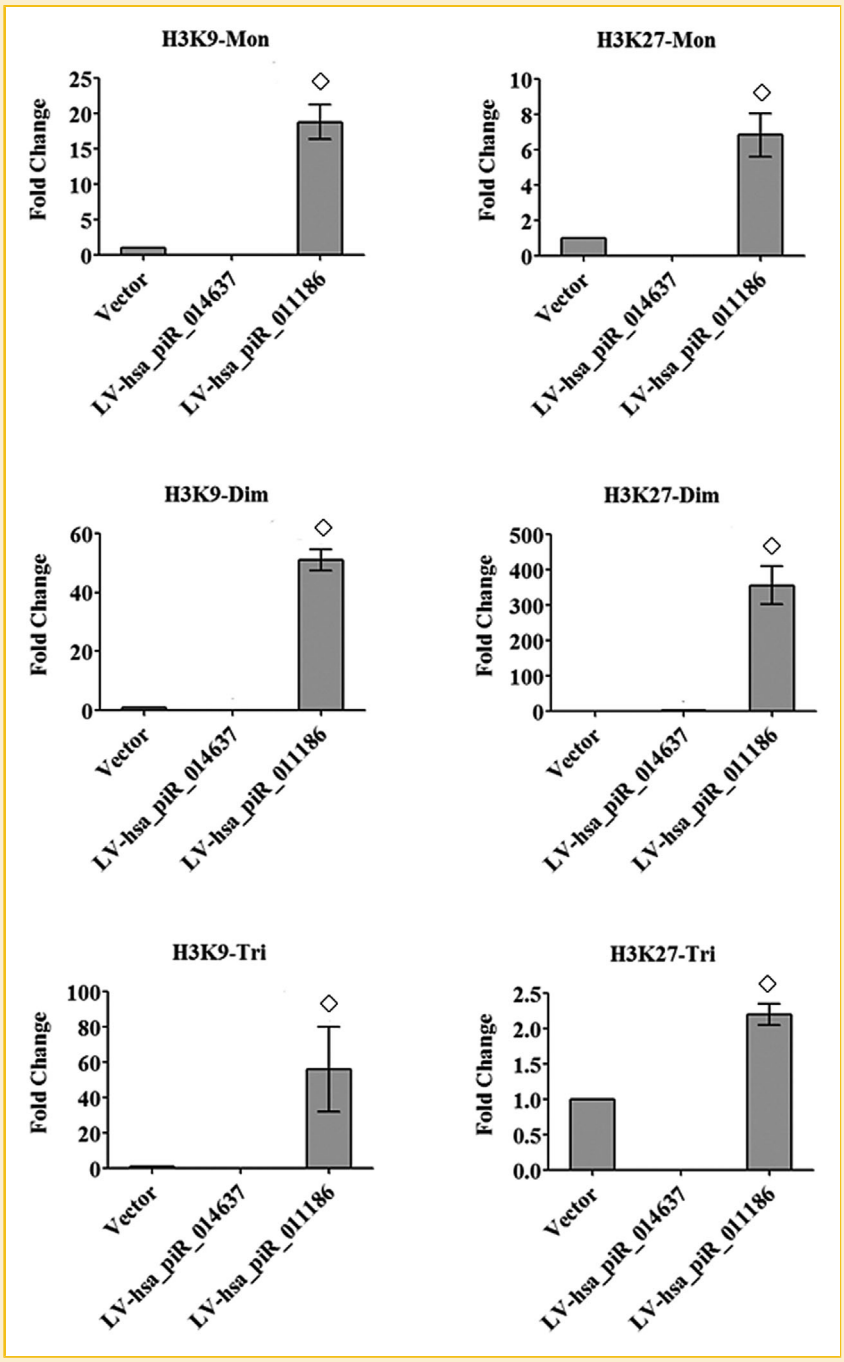

Fig. 5. Fold-change of ChIP-qPCR assay to detect methylated histones (H3K9,H3K27) at CDKN2B gene promoter in U937 human leukemia cells after infection. U937 cells were infected with Vector, LV-hsa_piR_014637 or LV-hsa_piR_011186 for 48 h. After infection, chromatin was prepared and assayed for methylation level of histones (H3K9 and H3K27) at CDKN2B gene promoter in U937 cells through ChIP assay. ChIP assay showing the levels of H3K9 (mono-, dim- and trimethylation) and H3K27 (mono-, dim- and trimethylation) at the promoter of the $p15^{INK4b}$ genes in the U937 cell lines after infection. Levels were determined by qPCR and are expressed as fold change ($2^{-\Delta\Delta Ct}$). The results represent mean ± standard deviation of three independent experiments (vector control group, LV-hsa_piR_014637 group and LV-hsa_piR_011186 group). Compared with vector control group, histone H3 at CDKN2B gene promoter region manifested different degree of methylation in K9 and K27 in LV-hsa_piR_014637 infection group and LV-hsa_piR_011186 infection group, especially in LV-hsa_piR_011186 infection group($P \leq 0.05$). Mann-Whitney U test, ◇ represents $P \leq 0.05$, vs control group. Mann-Whitney U test, ◇ represents $P \leq 0.05$, H3K9-Dim vs H3K27-Dim.

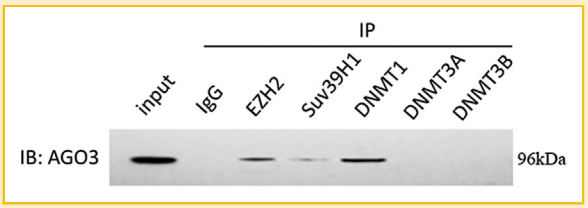

Fig. 6. AGO3 interaction verified by Co-IP assay in U937 human leukemia cells. Five interaction proteins (EZH2, Suv39H1, DNMT1, DNMT3a, and DNMT3b) were tested. Nuclear extract and nonspecific isotype IgG were used as input control and IgG Isotype control, respectively. The piRC member AGO3 protein in the six above-mentioned samples and the blank control sample were analyzed through Western blotting with AGO3 monoclonal antibody as primary antibody and HRP-labeled goat anti-mouse IgG antibody as secondary antibodies. piRNAs-AGO3 complexes contain DNA methyltransferase DNMT1 and histone methylase Suv39H1 and EZH2, but not DNA methyltransferases DNMT3a and DNMT3b.

the CpG islands within the CDKN2B promoter region. There was aberrant DNA methylation in the CDKN2B promoter area of the LV-hsa_piR_011186 transduced group (Fig. 4c). Methylation varied from the 2nd to the 44th CG spots in the CpG island. Each spot had a methylation rate above 20%, with a maximum 50% methylation rate in some specific spots (the 34th and 35th location). The vector control group (Fig. 4e) and LV-hsa_piR_014637 (Fig. 4d) transduction group displayed insignificant methylation modification in the CpG island of CDKN2B promoter region.

HETEROCHROMATINIZATION OF CDKN2B GENE PROMOTER REGION OF TRANSDUCED CELLS

The BSP method revealed methylation modification in the CpG island within the *CDKN2B* promoter region of the LV-hsa_piR_011186 transduction group. This modification resulted in the down-regulation of gene expression. There were no methylation modifications in the LV-hsa_piR_014637 transduction group, even though the group exhibited slight *CDKN2B* down-regulation in comparison with the vector only control group. Since heterochromatinization of a promoter region is also involved in the regulation of gene expression and may have contributed to CDKN2B down-regulation in the LV-hsa_piR_014637 transduction group, it was necessary to test the heterochromatinization status in the *CDKN2B* promoter region of transduced cells. ChIP-qPCR was used to assess histone H3 methylation in the *CDKN2B* promoter area. Compared to the vector control group the LV-hsa_piR_011186 transduction group displayed significantly different levels of histone H3 methylation ($P \leq 0.05$) (Fig. 5), whereas the LV-hsa_piR_014637 transduction group did not. In the hsa_piR_011186 transduction group, both H3K9 and H3K27 exhibited different levels of methylation including mono-, di- and trimethylation. The dimethylation of H3K27 was the most profound.

piRC COMPONENTS AND FUNCTIONAL FACTORS IN U937 LEUKEMIA CELLS

The data so far clearly indicate the formation and activity of piRNA complexes in U937 cells after the transduction of LV-hsa_piR_014637 and hsa_piR_011186. These complexes mediated down regulation of the *CDKN2B* gene through methylation. In order to identify the methyltransferases that were a component of the piRC, co-immunoprecipitation (Co-IP) was performed using antibodies against histone methyltransferases EZH2 and Suv39H1, and against DNA methyltransferases DNMT1, DNMT3a, and DNMT3b. The protein complexes were then captured by antibody-binding Protein G beads followed by elution of the antibody-bound proteins. In humans, AGO3 is known to associate with miRNAs in suppressing the translation of target mRNAs. To investigate the possibility of AGO3 association with piRNAs, Western blots were

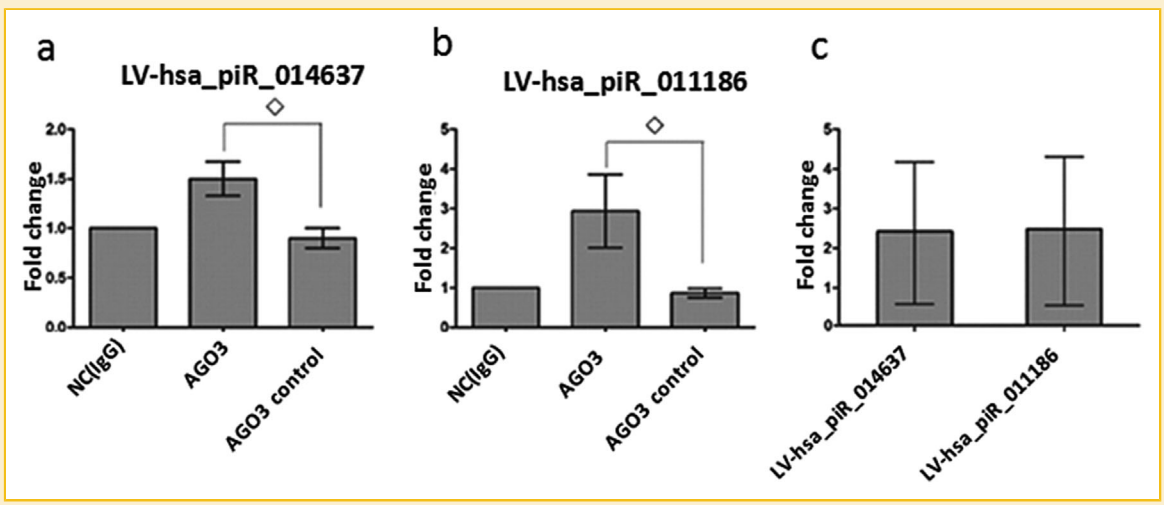

Fig. 7. Relative level of p15-piRNAs associated with AGO3 in U937 cells after infection. U937 cells were infected with vector, LV-hsa_piR_014637 or LV-hsa_piR_011186 for 48 h. RNA immunoprecipitation (RIP)-qPCR assay was performed to assess the level of piRNAs associated with AGO3. The results represent mean ± SD of three independent experiments, which showed the fold-change in site occupancy of hsa_ piR_011186 and hsa_ piR_014637 groups. Figures showed the data of LV-hsa_ piR_014637 infected group (a), LV-hsa_piR_011186 infected group (b), and the normalization data of two groups (c). Mann-Whitney U test, ◇ represents $P < 0.05$.

performed using anti-AGO3 monoclonal antibody. The results showed that AGO3 associated with DNMT1, Suv39H1, and EZH2, but not DNMT3A or DNMT3B proteins in U937 cells (Fig. 6). This suggests that a complex consisting of AGO3 and DNMT1, Suv39H1, or EZH2 was formed in U937 cells, and will be referred to as the piRNAs-AGO3 protein complex henceforth.

BINDING CAPACITY OF piRNA WITH AGO3

To test the binding of over-expressed piRNAs to endogenous AGO3 after transduction, RIP-qPCR was used 48 h after transduction in U937 cells. AGO3 binding by both piRNAs increased compared with the control group transduced with empty vector (Fig. 7a, 7b). After normalizing for the difference in the expression level of piRNA transduction (Fig. 7c), no significant difference was found in the fold change between the two piRNAs.

DISCUSSION

In this study, we investigated the role of hsa_piR_014637 and hsa_piR_011186 piRNAs on *CDKN2B* in epigenetic modification by over-expressing these two piRNAs in U937 cells. Both hsa_-piR_014637 and hsa_piR_011186 piRNAs are endogenously expressed in U937 cells, where hsa_piR_011186 is relatively more abundant. Although the mechanism of the differential expression levels remains unknown, the higher level of hsa_piR_011186 may be due to the structural stability of the piRNA itself. To investigate the function of the piRNAs in U937 cells, we explored cell proliferation and apoptosis in cells ced with piRNA overexpression plasmids. Both piRNAs facilitated proliferation, but only hsa_ piR_011186 inhibited cell apoptosis. These findings can be explained by the down-regulation of *CDKN2B* genes and p15 proteins in transduced cells.

To elucidate the mechanism of down-regulation of *CDKN2B* in transduced cells, the BSP method was used to analyze the methylation profiles of the 45 loci in the CpG island in the promoter region of *CDKN2B*. In the LV-hsa_piR_011186 transduction group, the CpG island in the *CDKN2B* promoter area was methylated to various extent, which in turn reduced mRNA transcription and *CDKN2B* expression. On the other hand, in the LV-hsa_piR_014637 transduction group, no methylation in the CpG island was found. However, based on the fact that heterochromatinization of promoter region also affects gene transcription, it's likely that histone H3 methylation in the promoter region induced transcriptional gene silencing. ChIP-PCR was used to assay for the heterochromatin levels in the promoter region of *CDKN2B* in transduced cells. In the LV-hsa_piR_011186 overexpression group, histone H3K9 and H3K27 in *CDKN2B* promoter region were subjected to different levels of methylation modification, where the most significant was the dimethylation in H3K27. Therefore, piR_011186-mediated *CDKN2B* silencing could be a result of the piRNA-binding to specific complementary sequence on the target gene, followed by the recruit of DNA and histone methyltransferases to the *CDKN2B* gene for epigenetic modification.

From our Co-IP and Western blot data, we were able to identify a DNA methyltransferase (DNMT1) and two histone methyltransferases (EZH2 and Suv39H1) that interacted with hsa_piR_014637 and hsa_piR_011186 in forming piRCs. Of particular interest is the finding that the piRCs consist of AGO3, a member of the human argonaute protein family. Moreover, by overexpressing the piRNAs, it was revealed that the binding affinities between both piRNAs and AGO3 were strong. Such unusual association between piRNA and argonaute proteins may occur in cancer biogenesis to disrupt gene expressin. Our results show that not only was AGO3 involved in the synthesis of piRNAs, it also facilitated epigenetic modifications. The methylation profile of LV-hsa_piR_011186 transduced group is indicative of de novo methylation. It's possible that DNMT3a and 3b, which mediate de novo methylation, associated with targeting proteins other than AGO3 to account for this observation. Another possibility is that the ectopic expression of LV-hsa_piR_011186 may have triggered some de novo methylation ability by DNMT1, even though DNMT1 normally prefers hemimethylated DNA.

Huang et al. [2013] reported a piRC complex formed by Piwi, HP1a and Su(var) 3–9 proteins that could catalyse the covalent modification of histones, similar to the piRCs in U937 cells. DNMT1, a cytosine C5-specific methyl transferase, is aberrantly expressed in tumor cells and facilitate tumorigenesis by triggering the hyper-methylation of promoter regions of tumor suppressor genes, creating an early molecular hallmark of tumor formation. The histone methylase Suv39 (suppressor of variegation 3–9) catalyzes the methylation of histone H3K9. Silencing Suv39H1 leads to the expression of *CDKN2B* gene and suppression of cell proliferation through de-methylation of H3K9 in the promoter region of tumor suppressor genes [Zhao et al., 2013]. EZH2 belongs to the PcG gene family and catalyzes histone H3K27 methylation. It's involved in regulating chromosome structure and gene expression [Knutson et al., 2012; Wang et al., 2012].

One limitation of this study is that we only used one cell line to investigate the mechanism. Evidences from additional cell lines will provide more convincing data. This limitation should be addressed in the following study.

In conclusion, LV-has_piR_011186 and not LV-hsa_piR_014637 appears to mediate the DNA and histone H3 methylation of the *CDKN2B* promoter region to affect the expression of *CDKN2B* gene and ultimately facilitated cell proliferation and inhibited apoptosis. The precise mechanism likely involves piRNA-binding to a specific complementary sequence, followed by the recruitment of DNA and histone-methylating proteins to the *CDKN2B* gene. Although piRNAs were first discovered in germ-line cells and served to preserve the integrity of the genome by inhibiting transposon activity, current evidence supports the notion that piRNA is also involved in tumorigenesis by down-regulating tumor suppressing genes or CDK inhibitors. The piRNA database lists 23,439 piRNA sequences in the human genome. Since the *CDKN2A* gene is located in chromosome 9p21 and is adjacent to the *CNKN2B* gene with a gap of only 8412 nucleotides, we will further investigate whether the two piRNAs under study could affect the expression of other proteins encoded by *CDKN2A/B*, for example, p16INK4A and p14-ARF. We believe that different sets of piRNAs are activated in and could even determine fates of different cell types. The mechanism and timing governing the diverse compositions of piRNA-protein complexes and the activation of cetain piRNAs in various kinds of cells is a subject that requires further clarification.

ACKNOWLEDGMENTS

This work was supported by Fujian Medical University (09-ZD021), National Natural Science Foundation of China (81370629 and 81300428), Natural Science Foundation of Fujian Province (2011J01179), Fujian Provincial Health Bureau Youth Research Projects (2010-1-12), and National Clinical Key Specialty Construction Project.

REFERENCES

Aravin A, Gaidatzis D, Pfeffer S, Lagos-Quintana M, Landgraf P, Iovino N, Morris P, Brownstein MJ, Kuramochi-Miyagawa S, Nakano T, Chien M, Russo JJ, Ju J, Sheridan R, Sander C, Zavolan M, Tuschl T. 2006. A novel class of small RNAs bind to MILI protein in mouse testes. Nature 442:203–207.

Ashe A, Sapetschnig A, Weick EM, Mitchell J, Bagijn MP, Cording AC, Doebley AL, Goldstein LD, Lehrbach NJ, Le Pen J, Pintacuda G, Sakaguchi A, Sarkies P, Ahmed S, Miska EA. 2012. PiRNAs can trigger a multigenerational epigenetic memory in the germline of *C. elegans*. Cell 150:88–99.

Bies J, Sramko M, Fares J, Rosu-Myles M, Zhang S, Koller R, Wolff L. 2010. Myeloid-specific inactivation of p15Ink4b results in monocytosis and predisposition to myeloid leukemia. Blood 116:979–987.

Bourc′his D, Bestor TH. 2004. Meiotic catastrophe and retrotransposon reactivation in male germ cells lacking Dnmt3L. Nature 431:96–99.

Brower-Toland B, Findley SD, Jiang L, Liu L, Yin H, Dus M, Zhou P, Elgin SC, Lin H. 2007. *Drosophila* PIWI associates with chromatin and interacts directly with HP1a. Genes Dev 21:2300–2311.

Chen CC, Wang KY, Shen CK. 2012. The mammalian de novo DNA methyltransferases DNMT3A and DNMT3B are also DNA 5-hydroxymethylcytosine dehydroxymethylases. J Biol Chem 287:33116–33121.

Cheng J, Deng H, Xiao B. 2012. PiR-823, a novel non-coding small RNA, demonstrates in vitro and in vivo tumor suppressive activity in human gastric cancer cells. Cancer Lett 315:12–17.

Cheng J, Guo JM, Xiao BX, Miao Y, Jiang Z, Zhou H, Li QN. 2011. PiRNA, the new non-coding RNA, is aberrantly expressed in human cancer cells. Clin Chim Acta 412:1621–1625.

Ender C, Meister G. 2010. Argonaute proteins at a glance. J Cell Sci 123: 1819–1823.

Foltankova V, Legartova S, Kozubek S, Bartova E. 2012. Tumor-specific histone signature and DNA methylation in multiple myeloma and leukemia cells. Neoplasma 59:450–462.

Girard A, Sachidanandam R, Hannon GJ, Carmell MA. 2006. A germline-specific class of small RNAs binds mammalian Piwi proteins. Nature 442:199–202.

Grivna ST, Beyret E, Wang Z, Lin H. 2006. A novel class of small RNAs in mouse spermatogenic cells. Genes Dev 20:1709–1714.

Halic M, Moazed D. 2009. Transposon silencing by piRNAs. Cell 138: 1058–1060.

Huang XA, Yin H, Sweeney S, Raha D, Snyder M, Lin H. 2013. A Major Epigenetic Programming Mechanism Guided by piRNAs. Dev Cell 24:502–516.

Ishizu H, Siomi H, Siomi MC. 2012. Biology of PIWI-interacting RNAs: New insights into biogenesis and function inside and outside of germlines. Genes Dev 26:2361–2373.

Knutson SK, Wigle TJ, Warholic NM, Sneeringer CJ, Allain CJ, Klaus CR, Sacks JD, Raimondi A, Majer CR, Song J, Scott MP, Jin L, Smith JJ, Olhava EJ, Chesworth R, Moyer MP, Richon VM, Copeland RA, Keilhack H, Pollock RM, Kuntz KW. 2012. A selective inhibitor of EZH2 blocks H3K27 methylation and kills mutant lymphoma cells. Nat Chem Biol 8:890–896.

Kusy S, Larsen CJ, Roche J. 2004. P14(ARF), p15(NK4b) and p16(INK4a) methylation status in chronic myelogenous leukemia. Leuk lymphoma 45:1989–1994.

Lau NC, Seto AG, Kim J, Kuramochi-Miyagawa S, Nakano T, Bartel DP, Kingston RE. 2006. Characterization of the piRNA complex from rat testes. Science 313:363–367.

Leslie M. 2006. Cell biology. The immune system′s compact genomic counterpart. Science 339:25–27.

Le Thomas A, Rogers AK, Webster A, Marinov GK, Liao SE, Perkins EM, Hur JK, Aravin AA, Tóth KF. 2013. Piwi induces piRNA-guided transcriptional silencing and establishment of a repressive chromatin state. Genes Dev 27:390–399.

Lippman Z, Martienssen R. 2004. The role of RNA interference in heterochromatic silencing. Nature 431:364–370.

Lu HL, Tanguy S, Rispe C, Gauthier JP, Walsh T, Gordon K, Edwards O, Tagu D, Chang CC, Jaubert-Possamai S. 2011. Expansion of genes encoding piRNA-associated argonaute proteins in the pea aphid: diversification of expression profiles in different plastic morphs. Plos ONE. 6:e28051.

Morris KV. 2008. RNA-mediated transcriptional gene silencing in human cells. Curr Top Microbiol Immunol 320:211–224.

Papageorgiou SG, Lambropoulos S, Pappa V, Economopoulou C, Kontsioti F, Papageorgiou E, Tsirigotis P, Dervenoulas J, Economopoulos T. 2007. Hypermethylation of the p15INK4B gene promoter in B-chronic lymphocytic leukemia. Am J hematol 82:824–825.

Shirayama M, Seth M, Lee HC, Gu W, Ishidate T, Conte D, Jr, Mello CC. 2012. PiRNAs initiate an epigenetic memory of nonself RNA in the *C. elegans* germline. Cell 150:65–77.

Siddiqi S, Matushansky I, . 2012. Piwis and piwi-interacting RNAs in the epigenetics of cancer. J Cell Biochem 113:373–380.

Siddiqi S, Terry M, Matushansky I. 2012. Hiwi mediated tumorigenesis is associated with DNA hypermethylation. PLoS ONE 7:e33711.

Siomi MC, Sato K, Pezic D, Aravin AA. 2011. PIWI-interacting small RNAs: The vanguard of genome defence. Nat Rev Mol Cell Biol 12:246–258.

Takeuchi S, Bartram CR, Seriu T, Miller CW, Tobler A, Janssen JW, Reiter A, Ludwig WD, Zimmermann M, Schwaller J. 1995. Analysis of a family of cyclin-dependent kinase inhibitors: p15/MTS2/INK4B, p16/MTS1/INK4A, and p18 genes in acute lymphoblastic leukemia of childhood. Blood 86: 755–760.

Wang C, Liu Z, Woo CW, Li Z, Wang L, Wei JS, Marquez VE, Bates SE, Jin Q, Khan J, Ge K, Thiele CJ. 2012. EZH2 Mediates epigenetic silencing of neuroblastoma suppressor genes CASZ1, CLU, RUNX3, and NGFR. Cancer Res 72:315–324.

Yin H, Lin H. 2007. An epigenetic activation role of Piwi and a Piwi-associated piRNA in *Drosophila melanogaster*. Nature 450:304–308.

Zaratiegui M, Martienssen RA. 2012. SnapShot: Small RNA-mediated epigenetic modifications. Cell 151.

Zhao T, Ma XD, Huang YQ. 2013. Experimental study of SUV39H1 gene specific siRNA in human leukemia cell line. Zhonghua Xue Ye Xue Za Zhi.34:49–54.